BEHAVIOR OF THE BURNING OF PMMA SHEETS BY PILOT IGNITION

M. MAMOURIAN, J.A. ESFAHANI, M. B. AYANI

Mechanical Engineering Department, Faculty of Engineering, Ferdowsi University of Mashhad
P. O. Box. 91775-1111, Mashhad, Iran
jaesfahani@gmail.com

ABSTRACT   To explore the flame spread mechanisms over the solid fuel sheets, downward flame spread over vertical PMMA sheets with thicknesses from 1.75-5.75 mm have been examined in the quiescent environment. The dependence of flame spread rate on the thickness of sheets is obtained by a simple one-dimensional heat transfer model. An equation for the flame spread rates based on the thermal properties and the thickness of the sheet by scale up method is derived from this model. During combustion, temperature within the gas and solid phases is measured by a fine thermocouple. The pyrolysis temperature, the length of the pyrolysis zone, the flame temperature, and thermal diffusivity of the solid are determined from the experimental data. Mathematical analysis has yielded realistic results. Although constant flame spread rates are not typical of fire environment, the model provides a useful formula to predict the rate of flame spread over any solid fuel sheet thickness.

INTRODUCTION

Polymers are used in nearly every commercial buildings, residential house, transportation vehicle, etc. Thus the majority of polymer containing end products (cables, carpets, furniture,…) must pass some type of regulatory test to help assure public safety from fire. To minimize their hazards, the burning behaviors and combustion mechanism should be understood. Polymethylmethacrylate (PMMA) is a transparent material and has excellent corrosion resistance. These advantages make it so popular and widely used in building, industry and the general consumer products market [1]. Therefore, attention is restricted to PMMA, whose properties are simpler and better understood than those of most other polymeric materials.

Flame spread over the surface of polymeric material is one of the problems in fire researching. Many mathematical and experimental models have been constructed to describe the process of flame spread over a solid fuel. The controlling mechanism of flame spread appears to differ with the surrounding conditions, such as the oxygen concentration [2], or the direction of the gas flow velocity relative to the direction of the flame spread [3,4]. The flame spread rate depends on the rate of heat transfer from the flame into the preheat region (unburned fuel). The estimation of the heat transfer not only through gas phase but also through solid phase is important for further

understanding. Gas phase conductive/convective heat transfer from flame to the solid fuel is the dominate path for downward flame spread [1, 5].

In order to estimate the rate of heat transfer, one needs to know the detail temperature profiles in the gas and solid phases. Esfahani and kashani [6], and Esfahani [7] determined the history of temperature in the solid and gas phases of the PMMA sample by a numerical model. Fernandes-Pello and Williams [8], Fernandes-Pello and Santoro [9], Hirano et al [10], and Krishna Murthy and Williams [11] measured the histories of surface and interior temperature of PMMA for horizontal flame spread by using of the thermocouples.

In the present work, the relation between the flame spread rate and the thicknesses over the thin solid sheets is studied by order of magnitude analysis and investigates the effects of the type of the heat flux on the flame spread rates. The temperature histories were obtained from chart recording of the fine thermocouple output. The thermal diffusivity of the gas was extracted from the temperature histories. Experimental results show a good agreement with the analytical results.

PHYSICAL MODEL

A sample of thin solid sheet fuel (PMMA) is burned with a slit burner from its top surface and is held in the quiescent environment at a fixed temperature T_∞. The sample is assumed to be very large in width and length so that, a one dimensional model is appropriate for spreading its behavior. The lengths of the sample are considered without expansion during combustion. The sample has thermal balance with the environment, which has the temperature T_∞.

The schematic of the physical problem is shown in Fig. 1. The reaction zone can be divided into three major parts: The initial (preheated zone), thermal decomposition and combustion zone. In the initial zone, preheating occurs mainly due to absorption of thermal energy and energy transferred through this region by conduction. The thermal decomposition zone, where the rapid thermal decomposition occurs, is due to the convection heat flux from combustion product to the sample. The main diffusion flame is formed over this zone which is called combustion zone. For the flame propagation, the most important processes take place in the thermal decomposition zone. The solid fuel situated ahead of the flame edge is heated from the ambient temperature to the pyrolysis temperature, T_p. When the temperature of the sample rises, bubbles form and the pyrolysis occurs. The pyrolysis temperature of most polymers is between 180-400 ^{o}C [4]. When the temperature of the layer exceeds to a pyrolysis temperature, the intensity of gasification is enough to form a diffusion flame. The combustion process occurs as long as the gaseous volatiles are intensively delivered into the reaction zone.

MATHEMATICAL MODEL

Figure 2 depicts a downward flame spread over a sheet of arbitrary thickness in a flame fixed coordinate at the foot of flame. The horizontal and vertical axis are indicated by x and y, respectively. On a fixed coordinate, there is a flow of solid fuel in the negative direction of y at the velocity of V_f.

SCALE UP

To identify the relevant time and length scales, attention is focused on the leading edge of the flame where the fundamental mechanism of any flame spread occurs. Three control volumes are investigated: the first region in the gas phase of size $W \times \delta \times L_g$, the second region in the thermal

decomposition zone of size $W \times \delta \times L_p$ and finally the third region in the solid phase of size $W \times \delta \times L_s$ are drown at this zone. W and δ are the sample width in the x direction and the thickness of the sample in the z direction, respectively. The length scales, L_g, L_p and L_s in the y direction is unknown at this point.

In the control volume of gas phase, the volatiles and oxidizer react to raise the gas temperature from pyrolysis temperature T_p to a characteristic flame temperature T_F. In the control volume of thermal decomposition, gasification occurred in the constant pyrolysis temperature T_p. Finally, in the control volume of solid phase, the temperature change from its initial temperature T_∞ at $y = L_s$ to the characteristic pyrolysis temperature T_p at the pyrolysis surface.
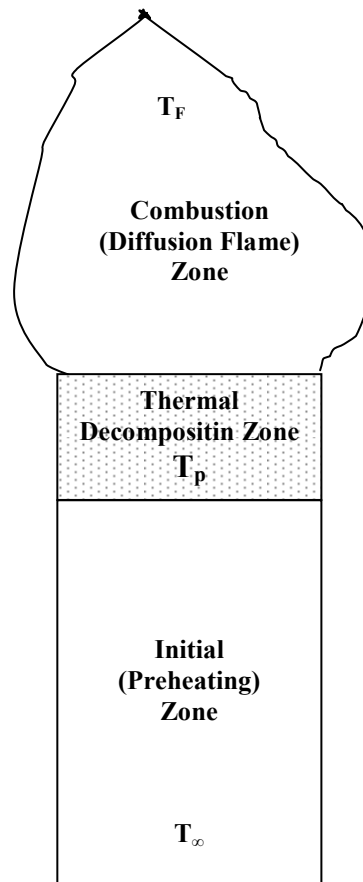

Figure 1. The schematic view of the combustion process in the solid sheet.

TIME SCALE:

There are three characteristic times that their scales are as follows, in the gas phase:

$$t_g \propto \frac{L_g}{V_g} \tag{1}$$

where V_g is the velocity of volatiles from the solid surface into the gas phase due to advection. The characteristic decomposition time, in the thermal decomposition:

$$t_p \propto \frac{Q_s}{q_p} \tag{2}$$

where Q_s and q_p are the maximum heat stored in the solid (J), and the heat consumed by the pyrolysis zone (W), respectively. In the solid phase:

$$t_s \propto \frac{L_s}{V_f}$$ (3)

where V_f is the flame spread rate. The flame spread is obtained based on a few simplifying assumption as follows [3]:
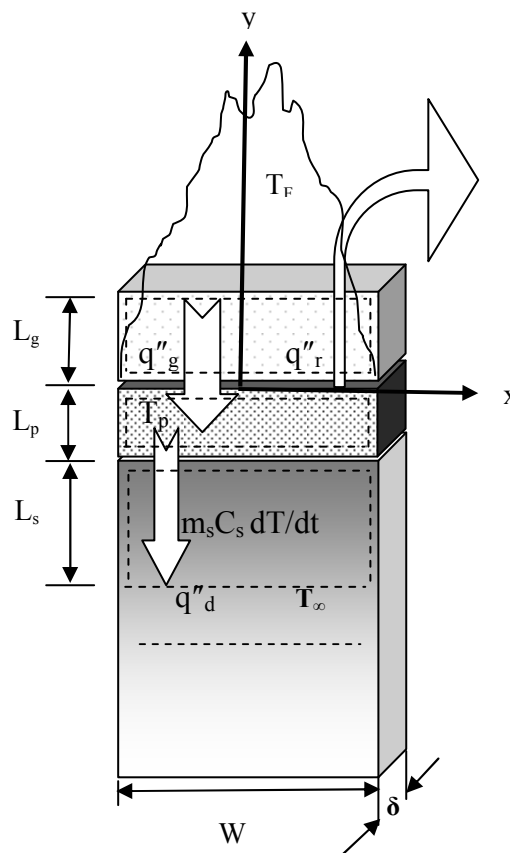

Figure 2. Control volume at the flame leading edge in the gas and solid phase.

- t_g is assumed to be large with respect to the characteristic chemical time justifying the assumption of infinitely fast chemistry.
- t_g is assumed to be small with respect to the radiative time scale justifying all neglected radiative effects.
- t_p is assumed to be small with respect to t_s allowing the use of a constant pyrolysis temperature.

The spread mechanism, therefore, is completely heat transfer limited and the resulting regime is generally called thermal regime.

LENGTH SCALE:

In the gas phase, L_g can be obtained as the diffusion length in the y direction within the available characteristic time [12]. Since $\partial T / \partial t \propto \alpha_g \partial^2 T / \partial y^2$, then L_g can be obtained as follows:

$$L_g \propto \sqrt{\alpha_g t_g} \tag{4}$$

By substituting Eq. (1) into Eq. (4):

$$L_g \propto \frac{\alpha_g}{V_g} \tag{5}$$

In the solid phase and in a similar manner, L_s can be obtained as follows:

$$L_s \propto \sqrt{\alpha_s t_s} \tag{6}$$

By substituting Eq. (3) into Eq. (6):

$$L_s \propto \frac{\alpha_s}{V_f} \tag{7}$$

Note that the spread rates and the velocity of volatiles are still unknown in these expressions. The spread rate obtained from an energy balance for the pyrolysis control volume of Fig.2 is obtained as follows:

$$q''_g = (q''_r + q''_d + q''_p) \tag{8}$$

where q''_g, q''_r, q''_d and q''_p are the diffusion heat flux that is penetrated from gas phase to the gasification surface, the radiation heat flux between the solid fuel and surrounding, the conduction heat flux diffused through the solid, and the heat flux that is consumed to degrade the solid phase, respectively. Each term and its order of magnitude in Eq.8 can be obtained as follows:

$$q''_g = -k_g \frac{\partial T_g}{\partial y} \propto k_g \frac{T_F - T_p}{L_g} \tag{9}$$

$$q''_r = \sigma \varepsilon_s (T_s^4 - T_{sur}^4) \propto \sigma \varepsilon_s (T_p^4 - T_\infty^4) \tag{10}$$

$$q''_p = m''_f h_v \text{ and } m'' = \int_0^\infty \rho_s A_s Exp(\frac{-E_s}{RT_s}) dy \tag{11}$$

$$q''_p \propto \rho_s A_s h_v L_p Exp(\frac{-E_s}{RT_p})$$

(12)

$$q''_d = -k_s \frac{\partial T_s}{\partial y} \propto k_s \frac{T_p - T_\infty}{L_s}$$

(13)

Scaling rules [13] implies q''_g and q''_d in Eq. (8) to be the same order:

$$k_g \frac{T_F - T_p}{L_g} \propto k_s \frac{T_p - T_\infty}{L_s}$$

(14)

If F_T defines $-\frac{T_\infty - T_p}{T_F - T_p}$ then:

$$\frac{L_g}{L_s} \propto \frac{1}{F_T} \frac{k_g}{k_s}$$

(15)

Due to mass conservation, reduced mass of the solid fuel equals the mass of volatiles; $m''_s = m''_v$ then:

$$V_f = \frac{\rho_g}{\rho_s} V_g$$

(16)

By substituting Eqs. 5 and 16 into Eq.15 and after rearranging, the flame spread rate can be estimated from the following relation:

$$V_f \propto F_T \cdot \frac{k_s}{\rho_s} \cdot \frac{1}{C_{p_g}} \cdot \frac{1}{L_s}$$

(17)

Due to previous observation for thin fuel $L_s \propto \delta$ [14, 15], which will be examined in the next section and if F_c defines C_s / C_{p_g} then, we have:

$$V_f \propto F_T \cdot F_c \cdot \alpha_s \cdot \frac{1}{\delta}$$

(18)

Since all of the parameters except V_f and δ are assumed to be constant, then the relation between V_f and $1/\delta$, is linear. This result is identical to the previous experimental work of Mamourian et al [14], analytical solution of Ayani et al [15], Suzuki et al [16], and Bhattacharjee et al [3]. The maximum value and the order of magnitude of energy flow (each term in Eq.8) can be calculated from the properties of table (1) and the results are listed in table (2). By comparing each term with the others, it is concluded that all of the terms have the same order, except the radiation one.

Therefore this term can be neglected in the energy balance which confirms the previous works [8, 17, 18]. By substituting the properties of PMMA into Eq. 18, it yields to:

$$V_f \propto 0.1077(\frac{1}{\delta})$$
(19)

The slope of the linear variation in this result (%4) is more than the slope of relation presented by Ayani et al [15]:

$$V_f = 0.1038(\frac{1}{\delta}) + 0.0347$$
(20)

Table 1 property of PMMA and the characteristic lengths.

Property	Value		Property	Value	
T_F (K)	1223	[3]	h_v (J/kg)	1.356×10^6	[20]
T_p (K)	673	[3]	E_s (J/mol)	1.33×10^5	[19]
T_∞ (K)	300		A_s (1/s)	2.92×10^9	[19]
k_s (W/m.K)	0.19	[3]	R (J/mol.K)	8.314	
k_g (W/m.K)	0.02624	[11]	ε_s (-)	0.9	[2]
α_s (m^2/s)	1.0644×10^{-7}	[3]	L_s (m)	2.87×10^{-3}	[*]
α_g (m^2/s)	2.19×10^{-5}	[11]	L_g (m)	0.36×10^{-3}	[*]
C_s (J/kg.K)	1500	[3]	L_p (m)	0.25×10^{-3}	[*]
Cp_g (J/kg.K)	1005	[11]	δ (m)	1.75×10^{-3}	

*Estimate from present work.

Table 2 the maximum value and the order of magnitude of energy flow

		Value (kW/m^2)	Order of magnitude
q_g''	$k_g \dfrac{T_F - T_p}{L_g}$	40.09	10
q_d''	$k_s \dfrac{T_p - T_\infty}{L_s}$	24.69	10
q_r''	$\sigma \varepsilon_s (T_p^4 - T_\infty^4)$	10	1
q_p''	$\rho_s A_s h_v L_p Exp(\dfrac{-E_s}{RT_p})$	50.11	10

EXPERIMENTAL SETUP

A schematic of experimental apparatus is shown in Fig. 3, according to ASTM 1356. Experiments were carried under the normal atmospheric conditions, $T_\infty = 300$ K, $P_\infty = 90$ Kpa. Sample PMMA sheets are made from various thicknesses of 1.75 mm to 5.75 mm. The sheets are made by Acrylic Enterprise Co., LTD. in Taiwan. The dimensions of the sample sheets are 150 mm high, 40 mm wide, set up vertically and ignites at the top edge by a pilot flame. A 25 μm wire diameter chromel-alumel thermocouple was used to measure the history of the temperature in solid and gas phases. The thermocouple is pressed into a hole which is drilled in the middle of the sample, about 40 mm under the top edge. At each time, the recorded data by thermocouple is entered to a computer. For each thickness, the test is repeated 3 times to minimize experimental errors.
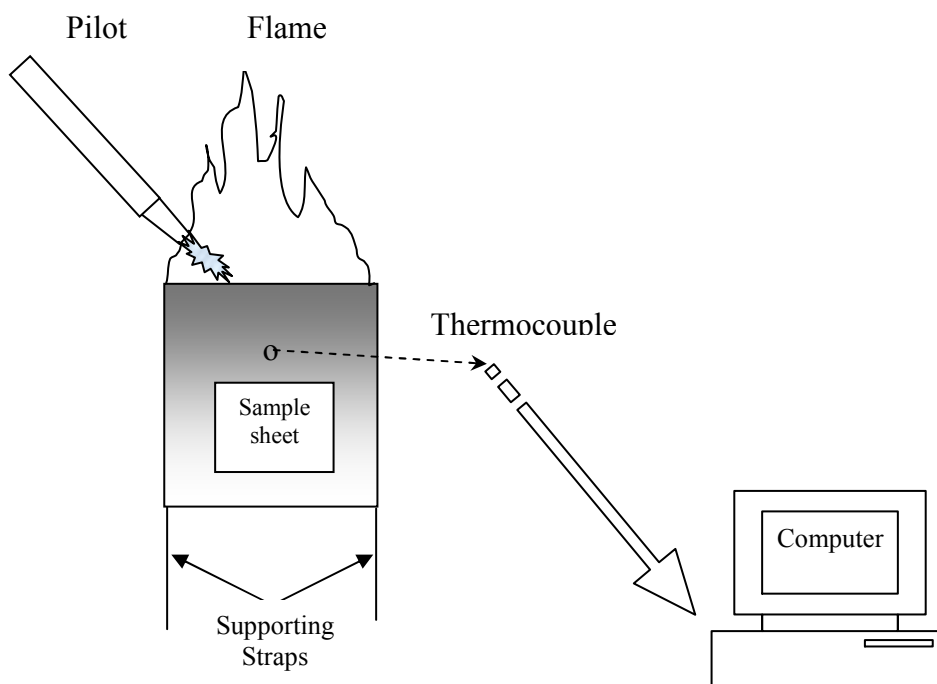

Figure 3. A schematic of the apparatus.

RESULTS AND DISCUSSION

The temperature distributions for various thicknesses of the sample are shown in Fig. 4. It shows that the solid temperature increases gradually (A-B), then it sharply increases (B-C) and reaches to a peak point (C), the pyrolysis temperature about 390 °C, then decreases slightly (C-D) and then jumps rapidly to a higher level (E). The release volatile of flammable gases moves to the outer atmosphere and mixes with air and absorbed thermal energy. Then the mixture ignites and the temperature in the gas phase increases. The temperature reaches to a maximum value of about 950 °C (G), and finally falls to the ambient temperature (H). These experimental data is about 7% less than the numerical previous works of Esfahani and Kashani [2, 6]. This may be, due to the

effect of radiation that was neglected in the previous numerical and analytical works [2, 6]. The interpretation of the history is the following. The first local maximum pyrolysis region (C), occurs when the junction of the thermocouple moves from the solid into a liquid-like layer adjacent to the surface of the sample. Thereafter, the properties of the sample change and, thereby accounting for the temperature to decrease. The first peak (C) and the sudden increase in the recorded temperature (E) provides lower and upper levels for the surface temperature (pyrolysis region) $T_{p,l}$ and $T_{p.u}$, respectively. The characteristic length L_p, defined in this level, is increased by increasing the thicknesses of the sample, and its order is proportional to the thicknesses. This result confirms the result of Fernandez-Pello and Williams, $L_p \propto \alpha_s / V_f$ [8]. The observed temperature jumps is due to tension in the junction into the gas phase. The fluctuations of measured temperature are due to variation of gas flow around the thermocouple. The smooth trace in the condensed phase (solid phase) seems to indicate that bubbling may not be a problem at high flame spread rates. At lower flame spread rates, due to the difference in the severity of the fluctuations between gas phase and condense phase, thermocouple location is less pronounced. Some-times observable fluctuations appear prior to the attainment of the first maximum temperature (C). These fluctuations are attributed to bubble formation in the liquid-like layer, a phenomenon which is known to occur at lower flame spread rates. The sharpness of increase of temperature varies from one test to another and may depend on fine details of the manner in which the thermocouple assembly is set into the sample. In some test the jump is difficult to discern, and the levels on the surface temperature are less certain. In these cases the first temperature peak is taken as the lower level, and the upper level is placed where gas phase fluctuations clearly become evident.
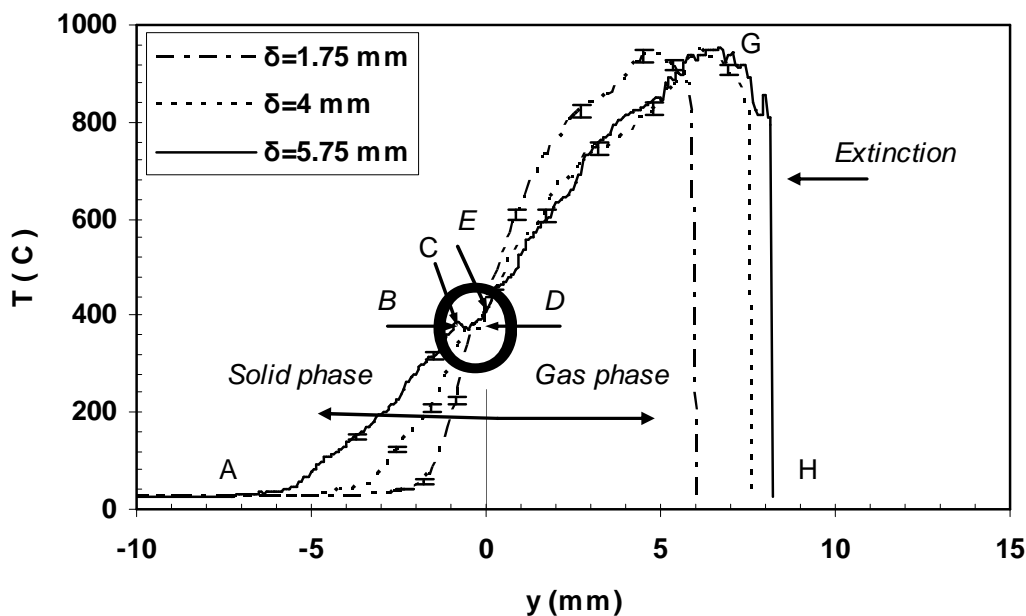

Figure 4. Temperature distribution in the solid and gas phase.

Conductive heat fluxes, q''_g and q''_d can be calculated by taking the spatial derivative of the temperature profile, shown in Fig. 4. The heat balance at the surface (y=0) with the assumption of negligible radiation can be expressed as follows [6, 21]:

155

$$-k_g \frac{\partial T_g}{\partial y} = -k_s \frac{\partial T_s}{\partial y} \tag{21}$$

The temperature distribution in the sample that is shown in Fig. 4 indicates that the high temperature zone (at the foot of flame) is located in the vicinity of the flame front. The values of each mode of heat flux based upon table (2), shows that the major part of net heat transfer rate into the sample is in this critical zone, and then the energy balance in this zone plays the major role for the flame spread rate. To simplify the modeling approach, the following assumptions were made:

- Steady state process.
- The temperature is uniform throughout the thickness of the sample.
- All thermal properties of the fuel sample are constant.
- Heat convection from the sample to the ambient is neglected.
- Movements of the volatiles within the solid (pre heat region) are neglected.

By use of the above assumptions, if Θ, Y and τ defines θ/θ_p, $-(y+L_p)/L_s$ and $\alpha_s t/L_s^2$, respectively, then the energy equation and boundary conditions in the solid phase can be expressed as follows:

$$\frac{\partial^2 \Theta}{\partial Y^2} = \frac{\partial \Theta}{\partial \tau} \tag{22}$$

$$Y = 0: \Theta = 1; \quad Y = 1: \Theta = 0; \quad \tau = 0: \Theta = 0 \tag{23}$$

where: $\theta = T - T_\infty$ and $\theta_p = T_{p,l} - T_\infty$

Since $V_f = -\dfrac{\alpha_s}{L_s} \dfrac{\partial Y}{\partial \tau}$, then Eqs. (22, 23) yield to:

$$\frac{\partial^2 \Theta}{\partial Y^2} = -\frac{V_f L_s}{\alpha_s} \frac{\partial \Theta}{\partial Y} \tag{24}$$

$$Y = 0: \Theta = 1; \quad Y = 1: \Theta = 0 \tag{25}$$

The non-dimensional temperature distributions for the various thicknesses of the sample in the solid phase are shown in Fig. 5. The thermal diffusivity of the solid can be determined from this curve, below the glass transition temperature (Θ about 0.2). The experimental value of α_s, can be estimated by use of Eq. 24 and the slop of the best linear curves of $\partial^2\Theta/\partial Y^2$ variation versus $\partial\Theta/\partial Y$ that is shown in Fig. 6. The value of α_s for PMMA that is predicted from this method is listed in table (3). Its average value is 1.1607×10^{-7} m^2/s. The value of α_s for PMMA in ref. [3] is 1.0644×10^{-7} m^2/s, that tits error is about 9%.
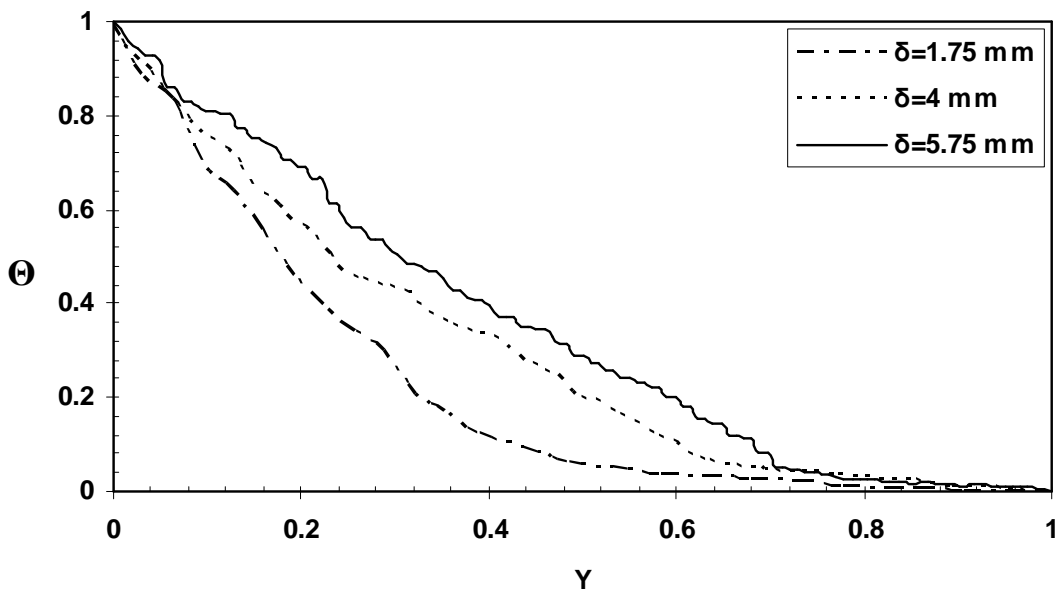
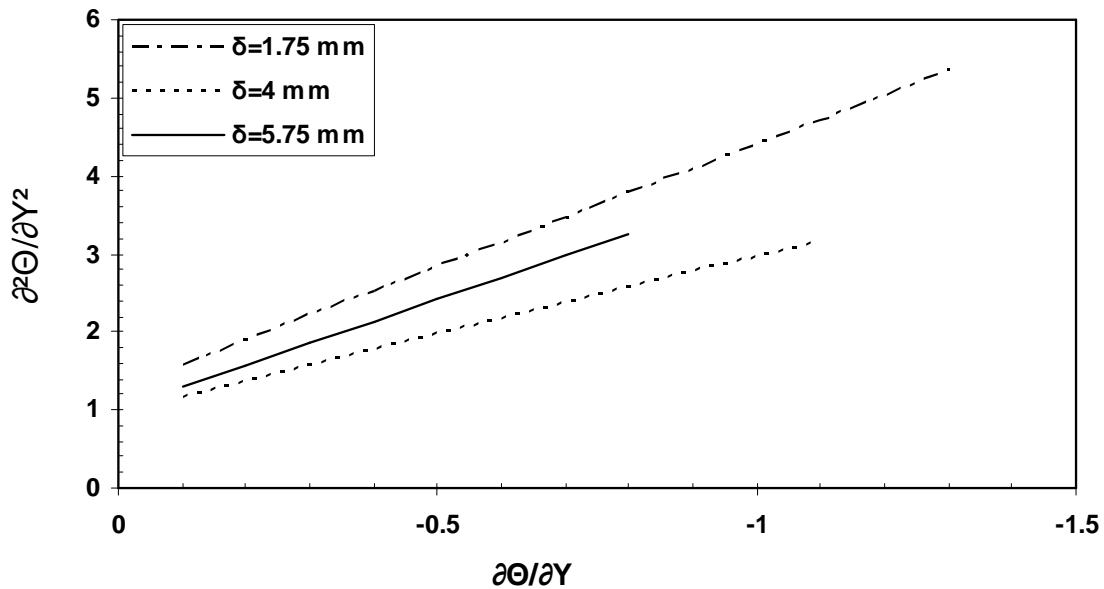Figure 5. Temperature distribution in the solid phase.

Figure 6. The variation of $\partial^2\Theta / \partial Y^2$ versus $\partial\Theta / \partial Y$ in the solid phase.

Table 3 Current experimental value of thermal diffusivity of the solid phase.

δ (mm)	V_f (mm/s)	α_s (m²/s)
1.72	0.098	0.9496×10^{-7}
4.00	0.060	1.3095×10^{-7}
5.75	0.053	1.2232×10^{-7}

CONCLUSIONS

An experimental study of downward flame spread along vertical sheet of PMMA was conducted. A simple analytical model, based on the scale up, was also adopted to explain the flame spread mechanism. This approach was reasonably successful in predicting the flame spread rates. The following conclusions can be drawn from the results obtained:

- The flame spread rate increased inversely with the decrease the thicknesses of the sheet.

- Since non-dimensional equations are used, it can be concluded that this method can be applied to other materials which have the physical behaviors like PMMA.

- The length of the pyrolysis increased with the increase in the thickness of sheet.

- The thermal diffusivity of solid phase could be determined from the slop of the linear curve that shows the variation of the second versus the first derivatives of the temperature history in the solid phase.

NOMENCLATURE

A	Zero order pre-exponential factor (s^{-1})
Cp_g	Specific heat of gas at constant pressure ($J.Kg^{-1}.K^{-1}$)
C_s	Specific heat of solid ($J.Kg^{-1}.K^{-1}$)
E	Activation energy ($J.Kg^{-1}$)
h_v	Enthalpy of volatiles ($J.Kg^{-1}$)
k	Thermal conductivity ($W.m^{-1}.K^{-1}$)
L	Length scale (mm)
m''	Rate of mass loss ($Kg.m^{-2}.s^{-1}$)
q	Consumed heat (W)
Q	Maximum heat (J)
q''	Heat flux ($W.m^{-2}$)
R	Gas constant ($J.Kg^{-1}.K^{-1}$)
T	Temperature (K)
t	Time scale (s)
V_f	Flame spread rate ($mm.s^{-1}$)
W	Width of sample (mm)

Greek letters

ρ	Density ($Kg.m^{-3}$)
ε	Emissivity (-)
α	Thermal diffusivity ($m^2.s^{-1}$)
δ	Thickness of sample (mm)
σ	Stefan-Boltzmann constant ($W.m^{-2}.K^{-4}$)

Subscripts

∞	Ambient
d	Diffusion
F	Flame
f	Fuel
g	Gas phase
p	Pyrolysis
r	Radiation
s	Solid
sur	Surround
v	Volatiles

REFERENCES

1. Zeng, W. R., Li, S. F. and Chow, W. K., Preliminary Studies on Burning Behavior of Poly methyl methacrylate (PMMA), *Fire Sciences,* 20 (2002)297-317.

2. Kashani, A. and Esfahani, J. A., Interactive effect of oxygen diffusion and volatiles advection on transient thermal degradation of poly methyl methacrylate (PMMA), *Heat and Mass Transfer,* 44 (2008) 641-650.

3. Bhattacharjee, S., Wakai, K. and Takahashi, S., Prediction of a critical fuel thickness for flame extinction in a quiescent microgravity environment, *Combustion and Flame,* 132 (2003) 523-532.

4. Fangart, J. and Wolanski, P., One dimensional analytical model of flame spread over solids, *Fire Sciences,* 9 (1991) 424-437.

5. Ito, A., and Kashiwagi, T.," Temperature measurements in PMMA during downward flame spread in air using holographic Interferometry", In: *21th Symposium (International) on combustion, The combustion Institute,* pp. 65-74, 1986.

6. Esfahani, J. A. and Kashani, A., One dimensional numerical model for degradation and combustion of polymethyl methacrylate, *Heat and Mass Transfer,* 42 (2006) 569-576.

7. Esfahani, J. A., Oxygen-sensitive thermal degradation of PMMA: a numerical study, *Combust. Sci. and tech.,* 10 (2002) 183-198.

8. Fernandez-Pello, A. C., and Williams, F. A., "Laminar flame spread over PMMA surfaces", In: *15th Symposium (International) on combustion, The combustion Institute,* pp. 217-231, Pittsburgh, Pennsylvania, 1975.

9. Fernandez-Pello, A. C., and Santoro, R. J., "On the dominate mode of heat transfer in downward flame spread", In: *17th Symposium (International) on combustion, The combustion Institute,* pp. 1201-1209, Pittsburgh, Pennsylvania, 1978.

10. Hirano, T., Koshida, T., and Akita, K., "Flame spread mechanisms over PMMA surfaces", In: *Bulletin of the Japanese Association of Fire Science and Engineering, pp.27- 1977.*

11. Krishnamurthy, L., and Williams, F.A., On the temperatures of regressing PMMA surfaces, *Combustion and Flame,* 20 (1973) 163-169.

12. Delichatsios, M. A., "Heat flux distribution in single vertical wall fires", In: *26th Symposium (International) on combustion, The combustion Institute,* pp. 1281-1293, Pittsburgh, 1996.

13. Bejan, A., *Convection Heat Transfer,* John Wiley and Sons, 2004.

14. Mamourian, M., Esfahani, J. A., and Ayani, M. B., The effect of the solid fuel dimensions on the downward flame spread, In: *2th Combustion conference of Iran (CCI-2),* pp. 250-259, Mashhad, 2008.

15. Ayani, M. B., Esfahani, J. A., and Mehrabian, R., Downward flame spread over PMMA sheets in quiescent air: experimental and theoretical studies, *Fire Safety,* 41 (2006) 164-169.

16. Susuki, M., Dobashi, R., and Hirano, T., "Behavior of fires spreading downward over thick paper", In: *25th Symposium (International) on combustion, The combustion Institute,* pp. 1439-1446, 1994.

17. Williams, F. A., "Mechanisms of fire spread", In: *16th Symposium (International) on combustion, The combustion Institute,* pp. 1281-1294, Pittsburgh, Pennsylvania,1978.

18. Fernandez-Pello, A. C., and Hirano, T., Controlling mechanisms of flame spread, *Combustion Science and Technology,* 1 (1983) 1-31.

19. Lengelle, G., Thermal degradation kinetics and surface pyrolysis of vinyl polymers, *AIAA, 8 (1970) 1989-1996.*

20. Krishnamurty, L., and Williams, F. A., "Laminar combustion of polymethyl methacrylate in O_2/N_2 mixtures", In: *14th Symposium (International) on combustion, The combustion Institute,* pp. 1151-1164, Pittsburgh, 1973.

21. Ayani, M.B., Esfahani, J.A., and Sousa, A. C. M., The effect of surface regression on the downward flame spread over a solid fuel in a quiescent ambient, *Thermal Science,* 11 (2007) 67-86.